

Prototype Demonstration of Nanosecond Optical Switching Based on REC-DFB Laser Array

Leilei Wang⁽¹⁾, Qi Sun⁽¹⁾, Zhewen Liu⁽¹⁾, WenHe Yin⁽²⁾, Zhenxing Sun⁽¹⁾, Tao Fang⁽¹⁾, Rulei Xiao⁽¹⁾, Mi Li⁽¹⁾, Yuan Du⁽²⁾, Li Du⁽²⁾, Chunhui Zhang⁽³⁾, Feng Wang⁽³⁾, Yashe Liu⁽³⁾, Xiangfei Chen⁽¹⁾

- (1) College of Engineering and Applied Sciences, Nanjing University, Nanjing 210093, Jiangsu, China, fangt@nju.edu.cn, chenxf@nju.edu.cn
(2) College of Electronic and Engineering, Nanjing University, Nanjing 210093, Jiangsu, China
(3) Huawei Tech. Co., Ltd., Shenzhen, China

Abstract We experimentally demonstrate a high-density monolithic integrated REC-DFB laser array chip with 100-GHz frequency spacing and less than 10 ns switching time, and a 2×2 optical switching prototype based on the chip and Arrayed Waveguide-Grating Router, achieving error-free transmission atop 25 Gbps NRZ per link with 12.8 ns end-to-end reconfiguration. ©2023 The Author(s)

Introduction

Driven by the ever-increasing 5G applications and emerging cloud workloads (such as HPC and DNNs), data traffic within data centers (DC) is forecast to grow exponentially. Today's DC networks comprise a hierarchy of electrical switches, interconnected using optical fibers, which will suffer from significant problems, such as high latency, poor scalability, low flexibility, high cost, and high energy consumption, etc. These aforementioned problems motivate the need for a new switching technology.

Optical switching combined with WDM technology could be an attractive alternative [1]. In particular, an optically-switched architecture based on fast wavelength tuneable source (WTS) and arrayed waveguide grating routers (AWGRs) [2-4] has received much attention recently due to its potential to create highly dynamic optical circuit switching connections, to efficiently handle small-packet DC workloads, as well as to improve the overall network resilience and simplify deployment by eliminating active elements in the network core.

WTS is the key component of optical switching networks, whose switching time determines the speed of physical-layer reconfiguration, and dwell time determines the minimum packet granularity. To meet the burst nature and high fan-out of DC traffic, a bandwidth-scalable WTS capable of nanosecond (ns) switching is necessary. There are mainly two types of WTS, Vernier-effect-based tuneable lasers via Bragg reflectors or micro-rings [5-6], and the tuneable distributed feedback multi-wavelength laser array (DFB-MLA) [7]. The on-off switching of the DFB laser on arrays is poised to provide extremely fast switching. The switching time is determined by the stable time of the relaxation oscillation, which is typically a sub-

nanosecond [8]. Besides, the DFB-MLA has high single-longitudinal-mode (SLM) stability and reliability as the common DFB lasers. Therefore, to achieve both high-speed wavelength switching and high SLM stability, the DFB-MLA is a good choice. However, the application of DFB-MLA is greatly limited by the number of laser integrations and precise wavelength spacing between lasers.

In this work, we designed and fabricated a monolithic integrated 16-channel DFB laser array based on the reconstruction equivalent chirp (REC) technique, which has average 100-GHz channel spacing under the same injected laser current. The laser's output power was above 10 mW, and the uniformity was within ± 0.5 dB. Based on the customized drive circuit board with a field-programmable gate array (FPGA), the 10%×90% rising/falling time between channels was less than 10 ns, which is independent of the wavelength span. Based on this chip and AWGR, 2×2 optical switching prototype experiments were conducted, and results showed that error-free transmission at 25 Gb/s NRZ per link was achieved with 12.8 ns end-to-end reconfiguration. The significance of the present work can be addressed in the following. (1) To the best of our knowledge, it should be the first demonstration of the ns-level optical switch based on DFB laser arrays. (2) Low-cost, large-scale, compact, and high-uniform channel spacing multi-wavelength laser may be very important for the true application of ultra-fast optical switching in the future.

Device Design and Fabrication

The REC technique is proposed to equivalently realize the complex grating structures by sampled grating [9]. Through predesigning the

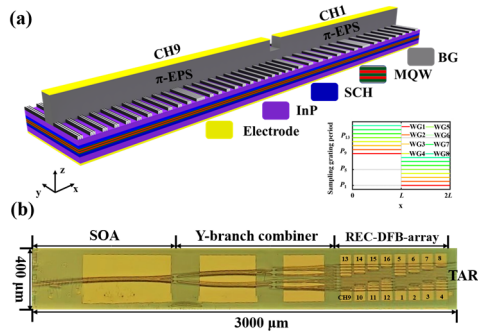


Fig. 1: (a) Schematic of the proposed 8-by-2 matrix laser array, (SCH-MQW: separate confinement hetero-structure-multi-quantum well; WG: waveguide); the right side: distribution of the sampling period along the eight parallel waveguides;(b) Microscopic top view of the proposed DFB-MLA.

sampled pattern, equivalent phase shifts and grating chirps are obtained in the high-order subgrating. The fabrication of the sampled grating requires only a common holographic exposure and μm -level photolithography. By using the REC technique, both the facility cost and fabrication time are lower than the conventional e-beam lithography technique. Moreover, the grating period variation error can be greatly relaxed by several hundred times theoretically, and DFB-MLA with high precision wavelength spacing can be achieved.

Sixteen π -shifted DFB lasers are arranged as an 8-by-2 matrix and denoted as CH1 to CH16, whose Bragg wavelengths meet ITU-T grids(C28-C43). The lasing frequency spacing of two in-series lasers at the same waveguide is 800 GHz, and the schematic is shown in Fig. 1(a). The right side of Fig. 1(a) shows the distribution of the sampling period along the eight parallel waveguides. For the tight arrangement of laser array, the distance of adjacent waveguides is designed to be $22 \mu\text{m}$, and a secondary electrode process is employed. The microscopic top view of the proposed DFB-MLA is shown in Fig.1(b). A

semiconductor optical amplifier (SOA) and a three-stage Y-branch combiner are monolithically integrated to obtain high fiber optical output power. The size of the chip is $400 \mu\text{m} \times 3000 \mu\text{m}$. The front and rear facets are both anti-reflections coated. The waveguides of both the tail absorption region (TAR) and the SOA are 7 degrees tilted to reduce the light reflection.

Device Characterization

The laser chip was mounted on a sub-mount, the temperature of which was controlled at 25°C via the temperature controller (TEC). The superimposed optical spectra and the side mode suppression ratios (SMSRs) of the 16 channels are shown in Fig. 2(a). The current injected into the SOA, the three-stage Y-branch combiner and the laser are 80, 50, and 50 mA, respectively. When one channel is lighted, the in-front lasers are injected with an appropriate current (transparent current) to compensate for the material absorption. Here, the transparent current is 15 mA. All the channels worked with good SLM operations with SMSRs of above 40 dB. We linearly fitted the lasing frequency of the 16 channels and calculated the frequency deviation. As shown in Fig.2(b), the average frequency spacing was 100 GHz, and the wavelength deviations of all 16 channels were within ± 20 GHz. Due to material refractive index deviation, arrays of accurate wavelengths could be realized slightly by adjusting the bias current of each laser to output a uniform wavelength comb, and then varying the TEC temperature to align all channels to the desired ITU-T grid. Typically, the threshold currents of two in-series lasers at the same waveguide were 22.4 mA, and 27.6 mA, respectively, as shown in the inset of Fig. 2(c). The output powers of all channels were above 10 mW with an SOA current of 110 mA, and the uniformity was within ± 0.5 dB, As shown

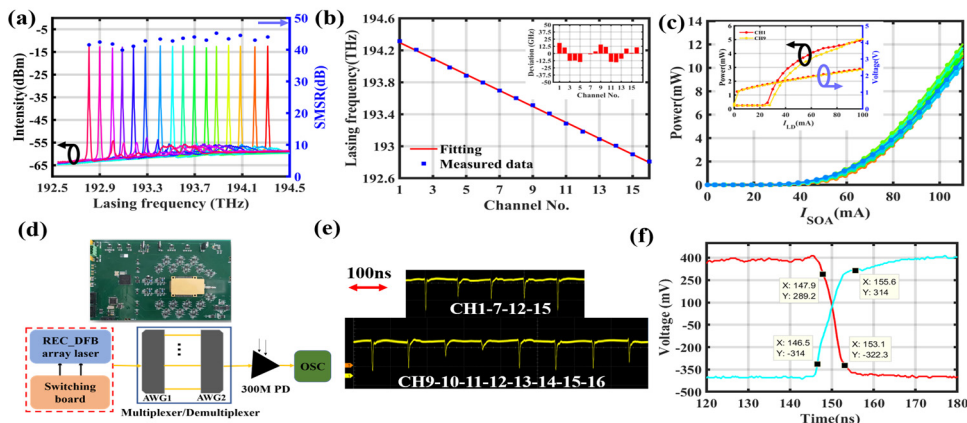


Fig. 2: (a) Measured superimposed spectra of the 16 channels; (b) Linearly fitting the lasing frequency, Inset: lasing frequency deviations; (c) Output power with respect to the I_{SOA} for all channels, Inset: a typical PIV diagram of the laser on the same waveguide; (d) Experimental setup for switching between channels;(e) 4 and 8 channels switching signals;(f) Intensity of the source and the destination channel during switching.

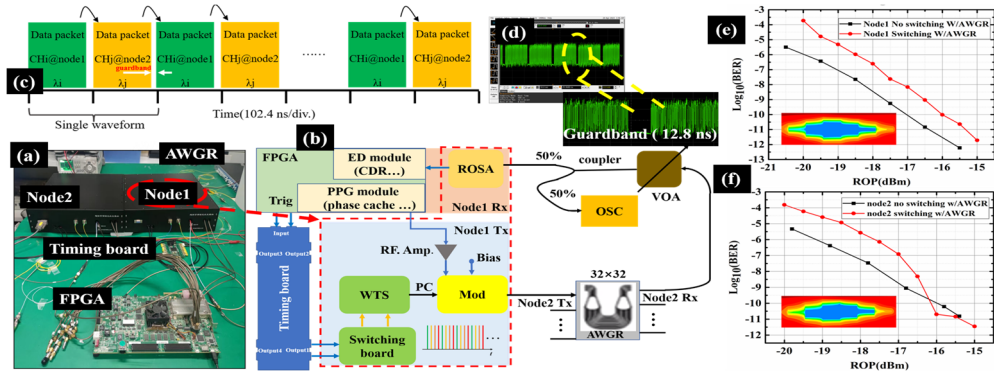


Fig. 3: (a) 2-node optical switching prototype. (b) Experimental setup of a node. (c) A stream of multiple burst data packets received by a cyclic schedule between the nodes; (d) Captured a stream of multiple burst data packets by real-time oscilloscope. (e-f) BER performance of each node.

in Fig. 2(c). The chip was packaged in a butterfly way to measure the switching speed using a driver board with an FPGA, as shown in Fig.2(d). For fast wavelength switching, the thermal effect is not a problem, as the thermal response times are much slower than the current variation. With the advent of wavelength routing, however, the dwell time at each wavelength is much longer, accordingly, thermal effects will impact the time during which the operating wavelength will be kept within receiver bandwidth. To solve the thermal problem, we adopted a relatively small injection current into the laser and shaped the driving current using pre-emphasis technology [10]. The selected channels in DFB-MLA were switched on in a round-robin manner, and the output was passed through a pair of arrayed waveguide grating (1-dB bandwidth is 0.18 nm) to a photodiode and the photodiode output was then captured by digital-sampling oscilloscope. As an example, a 4-channel and 8-channel switching was shown in Fig.2(e). The 10%×90% rise and fall times for each channel were shown in Fig. 2(f) with a maximum rise and fall time of 9.1 ns and 5.2 ns, respectively.

System Experimental Set-up and Results

As shown in Fig. 3(a), two-node optical switching prototype experiments were conducted to verify the performance of our proposed WTS. We used a high-performance FPGA with four sets of transceiver ports to emulate the nodes. As depicted in Fig.3(b), for node1, we connected the synchronous trigger signal of the FPGA to a timing board that enables all-node switching boards to keep the same pace. The high-speed transmitting port of node1 was connected to an external Mach-Zehnder modulator, operating at 25 Gbps burst-mode NRZ data sequences generated by FPGA. The modulated light was coupled into fiber and connected to an external AWGR. Depending on the wavelength, the AWGR redirects the signal that is from Tx of

node1/node2 under the corresponding burst slot to receiving port of node1 by the receiver optical subassembly (ROSA). To measure the end-to-end performance, the nodes transmitted burst-mode NRZ data to each other following a cyclic schedule. As shown in Fig.3(c), each burst is 102.4 ns at 25 Gbps, which is composed of 5 header packets (12.8 ns) to serve as a guard band and 35 payloads packets (89.6 ns). The ROSA received signal was captured on a 160 G Samples/s real-time scope, as shown in Fig.3(d); the 12.8 ns guard band was chosen to guarantee the WTS finishes switching with relatively constant amplitude. Meanwhile, the ROSA received signal was simulated by FPGA as shown in the inset of Fig.3(e-f)). BER measurements of the nodes were depicted in Fig.3(e-f). As a baseline, we also showed the BER measurements when no switching was performed. Results showed that error-free transmission ($BER < 10^{-12}$) was achieved at a receive optical power (ROP) of around -15 dBm.

Conclusion

A monolithically integrated 16-channel DFB laser array with average 100-GHz channel spacing under the same injected laser current has been fabricated. The laser's output power was above 10 mW, and the uniformity was within ± 0.5 dB. By on-off selected channels in a round-robin manner, the 10%×90% rise and fall times for each channel were measured to be less than 10 ns, which is independent of the wavelength span. Moreover, 2×2 optical switching prototype experiments were conducted, and results showed that error-free transmission at 25 Gb/s NRZ per link was achieved with 12.8 ns end-to-end reconfiguration. The present work is to pursue the practicability of ultra-fast optical switching. Further optimization of the REC-DFB-MLA chip is ongoing to design a more suitable package format for ultra-fast wavelength switching and to integrate modulators for low cost and small volume.

References

- [1] S. J. Ben Yoo, "Prospects and Challenges of Photonic Switching in Data Centers and Computing Systems," in *Journal of Lightwave Technology*, vol. 40, no. 8, pp. 2214-2243, 2022, DOI: 10.1109/JLT.2021.31365
- [2] Y. Yin, R. Proietti, X. Ye, C. J. Nitta, V. Akella, and S. J. B. Yoo, "LIONS: An AWGR-Based Low-Latency Optical Switch for High-Performance Computing and Data Centers," in *IEEE Journal of Selected Topics in Quantum Electronics*, vol. 19, no. 2, pp. 3600409-3600409, 2013, DOI: 10.1109/JSTQE.2012.2209174. 9
- [3] K. Shi et al., "System demonstration of nanosecond wavelength switching with burst-mode PAM4 transceiver," 45th European Conference on Optical Communication (ECOC 2019), Dublin, Ireland, 2019, pp. 1-4, DOI: 10.1049/cp.2019.1034.
- [4] Ballani, Hitesh, Paolo Costa, Raphael Behrendt, Daniel Cletheroe, István Haller, Krzysztof Jozwik, Fotini Karinou, Sophie Lange, Kai Shi, Benn Charles Thomsen, and Hugh Williams, "Sirius: A Flat Datacenter Network with Nanosecond Optical Switching," *Proceedings of the Annual Conference of the ACM Special Interest Group on Data Communication on the applications, technologies, architectures, and protocols for computer communication*, New York, USA, pp. 782-797, 2020, DOI:10.1145/3387514.3406221.
- [5] J. E. Simsarian, M. C. Larson, H. E. Garrett, X. Hong, and T. A. Strand, "Less than 5-ns wavelength switching with an SG-DBR laser," *IEEE Photonics Technology Letters*, vol. 18, no. 4, pp. 565-567, 2006, DOI: 10.1109/lpt.2005.863976.
- [6] S. Matsuo and T. Segawa, "Microring-Resonator-Based Widely Tunable Lasers," in *IEEE Journal of Selected Topics in Quantum Electronics*, vol. 15, no. 3, pp. 545-554, 2009, DOI: 10.1109/JSTQE.2009.2014248
- [7] K. Kudo et al., "1.55- μm wavelength-selectable microarray DFB-LD's with monolithically integrated MMI combiner, SOA, and EA-modulator," in *IEEE Photonics Technology Letters*, vol. 12, no. 3, pp. 242-244, March 2000, DOI: 10.1109/68.826901.
- [8] L. V. T. Nguyen, A. J. Lowery, P. C. R. Gurney, and D. Novak, "A time-domain model for high-speed quantum-well lasers including carrier transport effects," in *IEEE Journal of Selected Topics in Quantum Electronics*, vol. 1, no. 2, pp. 494-504, 1995, DOI: 10.1109/2944.401234.
- [9] Y. Shi et al., "Experimental demonstration of eight-wavelength distributed feedback semiconductor laser array using equivalent phase shift," *OPTICS LETTERS*, vol. 37, no. 16, pp. 3315-3317, 2012, DOI: 10.1364/OL.37.003315.
- [10] Zhiqian Yin, Qi Sun, Zhewen Liu, Yaguang Wang, Leilei Wang, Yunshan Zhang, Xingbang Zhu, Tao Fang, and Xiangfei Chen, "Nanosecond tunable laser for the all-optical switching network," *Applied Optics*, vol. 61, no. 34, pp. 10092-10097, 2022, DOI: 10.1364/AO.475633.